Sustainable Chemistry and Pharmacy 45 (2025) 102013

Contents lists available at ScienceDirect

Sustainable Chemistry and Pharmacy

journal homepage: www.elsevier.com/locate/scp

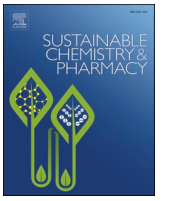

Exploring the potential of mealworm chitosan for hemodialysis applications

Maria Martingo, Sara Baptista-Silva, Raquel Mesquita, João Paulo Ferreira, Sandra Borges *, Manuela Pintado

Universidade Católica Portuguesa, CBQF - Centro de Biotecnologia e Química Fina – Laboratório Associado, Escola Superior de Biotecnologia, Rua Diogo Botelho 1327, 4169-005 Porto, Portugal

ARTICLE INFO

Handling Editor: Fabio Aricò

Keywords:
Tenebrio molitor
Chitosan
Bio-based membrane
Hemodialysis treatment

ABSTRACT

This study introduces a sustainable and efficient alternative to traditional chitosan sources derived from crustaceans, exploring the extraction and application of insect-derived chitosan from *Tenebrio molitor* for hemodialysis (HD) membranes design.

Efficient extraction and deacetylation methods were tested and developed between 6 h and 12 h to obtain chitosan. Chitin was isolated from *T. molitor* through deproteinization and demineralization, with yields of approximately 5 % (w/w). Chitosan was obtained from the extracted chitin resulting in yields of between 65.0 and 79.3 (w/w). Characterization using FTIR confirmed structural similarities with commercial chitosan and degrees of deacetylation in the 73–75 % range. The bioactive properties of chitosan obtained from *T. molitor*, including antimicrobial and antioxidant activities, were evaluated. All the microorganisms tested were inhibited, exhibiting minimum lethal concentrations between 2 and 8 mg/mL. In addition, chitosan showed antioxidant activity in the range of 60–65 μmol Trolox equivalent/g, suggesting its viability for various medical applications. This study additionally allowed the design of sustainable hybrid chitosan membrane (CH-M) tailored for HD applications. The permeation characteristics of CH-M for urea and albumin were studied in vitro to assess their suitability as HD membranes. Urea was permeable to values of over 70 % and albumin was retained. Also, cytotoxicity assays against L929 fibroblast cells demonstrated that the CH-M samples exhibit low metabolic inhibition (around 15 %) The application of CH-M in HD represents a significant advance, offering the potential for enhanced therapeutic outcomes for chronic kidney disease (CKD).

1. Introduction

The prevalence of CKD has been increasing over the years, presenting a growing public health challenge, and it is expected to become the 5th leading cause of death by 2040 (Foreman et al., 2018). The common therapeutic approach is HD, an extracorporeal treatment, usually administered 3 times a week for 3–4 h each time and employing semipermeable membranes. Extensive research has been dedicated to the design and development of these membranes, aiming to enhance the speed and efficiency of dialysis processes (Fox and Franklin). However, to date, sustainability and possible reuse have not been a priority or concern in current scientific advances. More than 90 % of dialysis membranes are fabricated from polysulfone (PSu) or polyethersulfone (PES). Udel® PSu and

* Corresponding author.
E-mail address: sandraferreiraborges@gmail.com (S. Borges).

https://doi.org/10.1016/j.scp.2025.102013
Received 6 December 2024; Received in revised form 11 March 2025; Accepted 31 March 2025
Available online 4 April 2025

Veradel® PES have emerged as the preferred polymers for crafting these membranes (Hestekin et al., 2023). Nevertheless, due to their plastic composition, these membranes are synthetic, non-biodegradable and designed for single use. This imposes an environmental strain worldwide, particularly evident in the estimated 4.1 million dialysis procedures conducted annually (Fresenius Medical Care, 2023). Modern HD filters are also made of hollow fibers produced via electrospinning, which must efficiently permeate and retain key biochemical markers in the blood, functioning as artificial kidney systems. These markers include urea and creatinine. In terms of urea, post-dialysis levels aim to be below 100 mg/dL, with creatinine levels decreasing to around 7–12 mg/dL. These fibers must also permit selective filtration while preserving essential blood proteins, such as albumin, which should remain within a physiological value of approximately 5.0 g/dL. The semipermeable nature of the dialysis membranes is crucial, allowing for the diffusion of waste products like urea and creatinine while preventing the passage of larger molecules (Bowry and Chazot, 2021).

The current investigation uniquely pioneers the study of the feasibility of using chitosan derived from edible insects, particularly *T. molitor*, as a main component of dialysis membranes to promote a new bio-hybrid concept for HD. *Tenebrio molitor*, a species of darkling beetle commonly known as the yellow mealworm is commercially available and already used in various food products and for personal consumption (EFSA Panel on Nutrition et al., 2021), which underscores the practicality and accessibility of this resource for medical applications. Also, *T. molitor* and other insects have, overall, a larger production of chitin material than crustaceans (Zainol Abidin et al., 2020). Chitin (poly (β-(1 → 4)-N-acetyl-D-glucosamine), is valued for its several key properties, including biodegradability, biocompatibility, and non-toxicity (Aberoumand and Chabavi, 2024). It serves as the exoskeleton's primary building block and is produced when mealworm larvae transform into pupae.

Chitosan is a biopolymer composed of glucosamine and N-acetylglucosamine units (Ravi Kumar, 2000) typically produced by the deacetylation of chitin, which involves the removal of the acetyl groups from the N-acetylglucosamine units (Kumirska et al., 2011). Chitosan, recognized for its significant bioactivity, is a biodegradable polymer that can be chemically modified to synthesize a variety of derivatives, thereby broadening its utility in diverse biomedical applications (Aberoumand and Muolenejad, 2024). Chitosan from insects is widely available because of its high reproductive rate, easy reproduction, and higher tolerance to environmental changes. Furthermore, it requires more moderate conditions of extraction, compared to the ones required for crustaceans. Due to its anti-coagulant (Bhattarai et al., 2010), anti-inflammatory (Edo et al., 2024), and antibacterial properties (Szymańska and Winnicka, 2015), chitosan may lower the chance of coagulation, inflammation, and/or infection in subjects undergoing dialysis. These upvalues properties make it a viable opportunity for future study and advancement in dialyzer technology, even raising avenues for possible reuse of membranes, given their antimicrobial potential.

To address these challenges, there has been a growing interest in developing alternative materials that are both sustainable and biocompatible (Kumar Gupta et al., 2015). Traditional materials such as PSu and PES, while effective in terms of performance, fall short on environmental sustainability and biocompatibility (Hestekin et al., 2023). The search for alternative materials has led to the consideration of biopolymers like chitosan, which offers several advantageous properties such as biodegradability, non-toxicity, and the ability to be chemically modified (Aberoumand and Chabavi, 2024). These properties may be crucial for medical applications, especially in a new era of HD where the biodegradability, reuse and biocompatibility of membranes with blood components are a step-forward vision (Bonomini et al., 2022). Chitosan derived specifically from mealworms, such as *T. molitor*, offers distinct advantages over other sources. The choice of mealworm-derived chitosan is strategic, leveraging its high yield of chitin, the precursor to chitosan, which surpasses that available from traditional marine sources. This not only reduces dependency on marine ecosystems but also aligns with more sustainable agricultural practices (Mei et al., 2024) given the lower environmental impact of farming mealworms compared to traditional livestock or marine harvesting (Safavi et al., 2024).

This study represents a groundbreaking advance in medical technology, as it is the inaugural effort to utilize chitosan derived from *T. molitor* for the development of HD membranes. This innovative approach not only introduces a sustainable source of biomaterials but also enhances the biodegradability and efficiency of membranes used in critical healthcare treatments. By integrating insect-derived chitosan into HD applications, this research sets a new standard for the incorporation of eco-friendly and high-performance materials in the healthcare industry.

2. Materials and methods

2.1. Materials

All standards and reagents, including commercial chitosan of medium molecular weight (approximate degree of deacetylation of 75 %, viscosity-based molecular weight of 190,000–310,000 Da) were obtained from Sigma-Aldrich (Sintra, Portugal), unless otherwise noted.

2.1.1. Microbial strains used for antimicrobial activity tests

For the antimicrobial assays, *Staphylococcus aureus* (MRSA, DSM 11729), *Candida albicans* (DSM 3454), and *Staphylococcus epidermidis* (DSM, 20044) were provided by DSM Pharmaceuticals Inc. (Durham, North Carolina, USA) and *Escherichia coli* (ATCC 25922), *Staphylococcus aureus* (MSSA, ATCC 29213) and *Pseudomonas aeruginosa* (ATCC 10145) were provided from American Type Culture Collection (Manassas, Virginia, USA). These strains were used as referenced nosocomial agents.

2.1.2. Cell lines growth conditions

A mouse fibroblast cell line, L929, was used (ECACC, U.K.). In the context of HD, fibroblasts can contribute to the study of cellular responses to biomaterials used in dialysis membranes (Biagini et al., 1994), focusing on extracellular matrix interactions and cellular

viability. The cells were grown as monolayer cultures in Dulbecco's Modified Eagle Medium (DMEM; Sigma Aldrich, Germany), which was enhanced with 1 % (10,000 U/mL) penicillin/streptomycin (Gibco, U.K.) and 10 % (w/v) fetal bovine serum (FBS; Biochrom, Germany). At 37 °C, the cells were cultured in a CO_2 incubator with a 5 % CO_2 environment, for 24 h.

2.2. Chitin and chitosan extraction

The samples of *T. molitor* larvae (Gotanbug, Portugal) were grinded to obtain a powder. To extract the chitin and chitosan from the *T. molitor* powder, the method presented by Shin et al. (2019) was used with modifications.

2.2.1. Chitin extraction

Two processes were tested varying the extraction time. In each, the dried insect powder (20 g) was subjected to alkaline treatment, with 10 % (w/v) NaOH solution (Merck, Darmstadt, Germany), at 90 °C, for 2 h (E4), or 4 h (E8), to remove protein, fat, and colour. The samples obtained were washed in distilled water until the pH value became neutral. Subsequently, samples were acid-treated with 7 % (v/v) HCl solution (Merck, Darmstadt, Germany), at 55 °C, for more than 2 h (E4) or 4 h (E8), respectively, to remove minerals, and then they were washed with distilled water until the pH value became neutral. After drying in an air oven at 60 °C for 24 h, chitin was obtained, with a colour corresponding to a light brown in both samples (E4 and E8). The overall procedure is schematically represented in Fig. 1.

After weighing the dried chitin, the yields were calculated according to the following equation (Eq. (1)) (Shin et al., 2019):

$$yield\ of\ chitin\ (\%) = \frac{weight\ of\ chitin}{weight\ of\ insect} \times 100 \quad (1)$$

2.2.2. Chitin deacetylation into chitosan

Two processes were performed, varying the deacetylation time. To remove the acetyl groups, the powder of each chitin sample (E4 and E8) from *T. molitor* was treated with a 55 % (w/v) NaOH solution, at 90 °C, for 2 h (E4D2 and E8D2), or 4 h (E4D4 and E8D4), and it was washed with distilled water until the pH value became neutral (Fig. 2).

After drying in the air oven at 60 °C for 24 h, the weight of the dried chitosan was evaluated, and the yields of the procedure were calculated according to the following equation (Eq. (2)) (Shin et al., 2019):

$$yield\ of\ chitosan\ (\%) = \frac{weight\ of\ chitosan}{weight\ of\ chitin} \times 100 \quad (2)$$

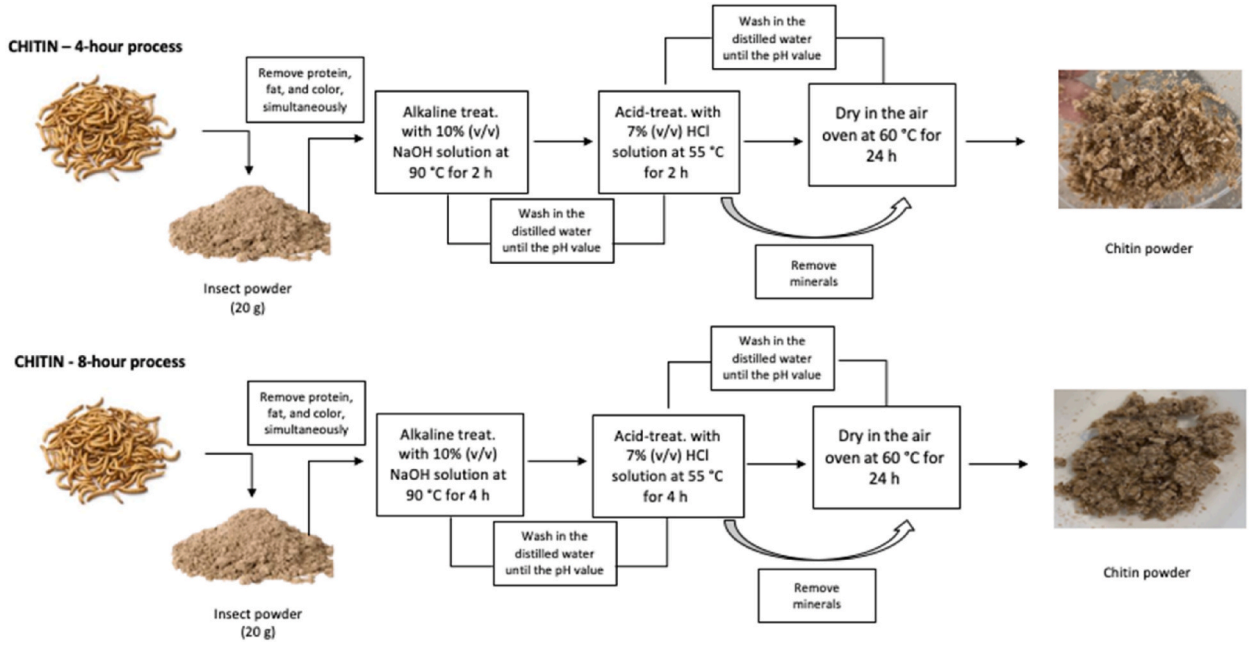

Fig. 1. Chitin extraction processes (i.e. extraction during 4 h and 8 h).

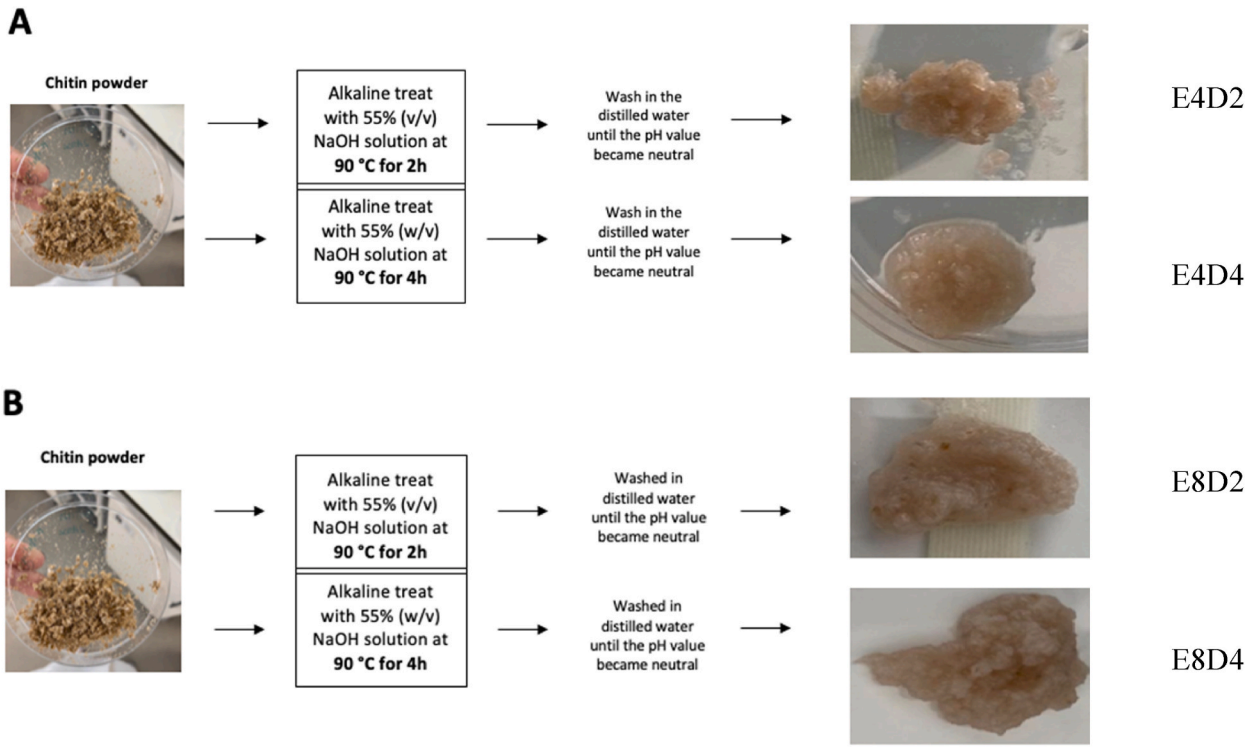

Fig. 2. Chitin deacetylation for chitosan extraction - (A) chitin powder, E4; (B) chitin powder, E8.

2.3. Chitosan physicochemical characterization

2.3.1. Fourier transform infrared spectroscopy

The extracted chitin and chitosan specimens underwent analysis through Fourier-transform infrared spectroscopy (FTIR-ATR analysis), utilizing a PerkinElmer spectrometer (Waltham, MA, USA) equipped with a diamond/ZnSe crystal and an attenuated total reflectance (ATR) sampling accessory from PIKE Technologies (Beaconsfield, UK). Each sample underwent 32 scans, covering the wavenumber range of 600–4000 cm^{-1}, with a spectral resolution of 4 cm^{-1}. Additionally, baseline point correction and spectra normalization procedures were implemented.

The degree of deacetylation (DD) in the chitosan samples was determined via the absorbance ratio (A1655/A3450), as the two parameters exhibit a linear correlation. The following equation was employed for DD calculation (Eq. (3)) (Czechowska-Biskup et al., 2012):

Degree of deacetylation (%): 97.67 - [26.486 x (A1655/A3450)] (3)

2.3.2. Dynamic light scattering and zeta potential

10 mg of extracted and commercial chitosan were dissolved in 1 % (v/v) acetic acid solution. The sample zeta potential (ZP) was evaluated with a NanoZSP device (Worcestershire, UK) (Coscueta et al., 2021). All tests were performed using a disposable foldable capillary cell with a 90° laser angle (Malvern, Worcestershire, UK) at room temperature (25 °C).

2.4. In vitro bioactivities of the extracted chitosan

2.4.1. Antioxidant activity

The antioxidant activity was assessed using the 2,2-azinobis-3-ethylbenzothiazoline-6-sulfonic acid (ABTS) radical as a photometric technique. The fundamental principle underlying ABTS involves the attenuation of a well-established metastable radical (ABTS+) by antioxidant compounds. The experimental procedure, as detailed in Coscueta et al. (2020), was executed in a 96-well microplate format. The assay was conducted using a multidetector plate reader (Synergy H1, Vermont, USA), operating under the guidance of Gen5 Biotek software version 3.04. To generate the ABTS radical cation (ABTS•+), a reaction mixture of 2.45 mM potassium persulfate and 7 mM 2,20-azinobis (3-ethylbenzothiazoline-6-sulfonic acid) diammonium salt was prepared. An absorbance of 0.70 ± 0.02 at 734 nm was maintained, achieved by combining 180 μL of the ABTS•+ working solution with 20 μL of either the sample or Trolox for the standard calibration curve (ranging from 25 to 175 M).

The scavenging activity for the control was expressed as a percentage reduction in absorbance. Trolox concentration was determined through regression equations, and the results were presented in units of μmol TE (Trolox equivalent) per gram.

2.4.2. Antimicrobial activity

Each microbial culture was grown aerobically in Muller Hinton agar (Biokar, France), for 24 h, at a temperature of 37 °C. The assays were conducted using a 1 % (v/v) acetic acid solution, which facilitated the dissolution of chitosan, and the pH of the solution was maintained at approximately 4.5. The bacteria were then moved to a sterile saline solution, and their turbidity was adjusted to 0.5 MacFarland scale, which is equivalent to an optical density of 0.08–0.1 at a wavelength of 600 nm. Dilutions within a concentration range of 1–10 mg/mL of commercial and extracted chitosan were prepared in Muller-Hinton broth. The chitosan solutions were then mixed with 2 % (v/v) of each microbial inoculum, and the resultant mixtures were incubated at 37 °C for 24 h. These inoculum-containing chitosan solutions were then placed onto Muller Hinton agar plates and kept incubating for an additional 24 h at 37 °C. Controls were included, such as the growth of microorganisms in a culture medium without insect chitosan and the inhibition of microorganisms with commercial chitosan with recognized antimicrobial activity.

The lowest chitosan concentration at which the initial viability of the microbial population was reduced by at least 99.9 %, was identified as minimum lethal concentration (MLC).

2.5. Design and development of a bio-based HD membrane

The method of chitosan extraction E4D2 was chosen, since it was the fastest, and with the best antimicrobial and antioxidant activities.

For membrane production, a 2 % (w/v) solution of polyvinyl chloride (PVC) in tetrahydrofuran was prepared, and then E4D2 chitosan powder was added to 1 % (w/v) concentration. This solution was mixed until becoming homogeneous (Rose et al., 2022).

The PVC/chitosan solution was transferred to a Petri dish and was left to dry at room conditions. After the membrane was dried, it was cut into approximately 6 × 1 cm rectangles.

2.5.1. Diffusion and retention parameters for permeation studies to simulate HD

The semi-permeability of CH-M was evaluated with a permeation study of urea and albumin. The goal was to understand the ability of the membrane to selectively allow the passage of certain molecules (urea) while restricting others (albumin), which is fundamental to its HD application. Solutions were propelled by a Gilson Minipuls 3 peristaltic pump with PhthalateFREE® PVC pump tubes (Fig. 3) to simulate the HD process.

The membrane was placed between the two chambers of equal volume (Fig. 4).

One of the chambers, the donor chamber, was filled with a solution of either urea at 37 mg/dL, or albumin at 8 g/dL). The other chamber was filled with deionised water (Mesquita and Rangel, 2005) (Fig. 5).

At appropriate time intervals (2, 4 and 6 min), a 1.5 mL sample from the donor chamber was collected, and the quantification of the solute diffused through the membrane was determined. For urea, a direct UV spectrophotometric assay, at 200 nm, was used. The linearity of the method was verified by constructing a calibration curve with a serial dilution of a standard urea solution at 37 mg/dL. For the quantification of albumin, the Pierce BCA Protein Assay Kit (Thermo Fisher, USA) was used.

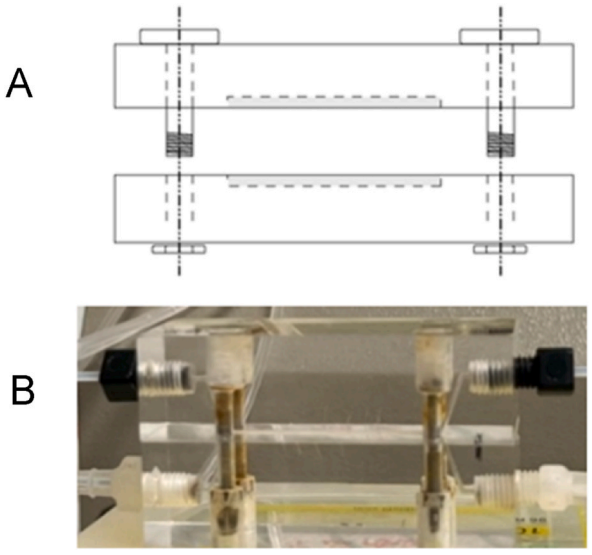

Fig. 3. (A) Scheme of lateral view of the configuration of the chambers (Mesquita and Rangel, 2005); (B) Lateral view of the chambers without the membrane.

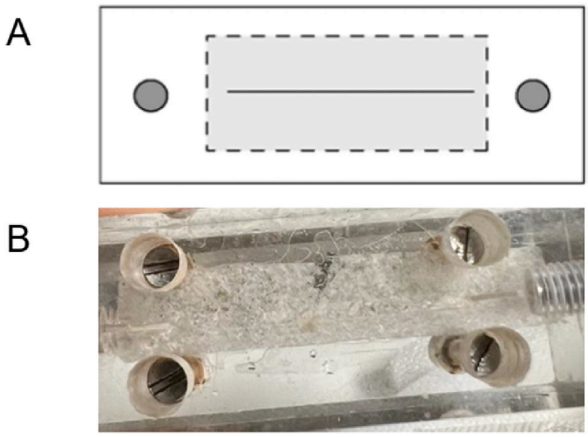

Fig. 4. (A) Scheme of top view of the configuration with a straight channel, length = 7.5 cm; (B) Top view of the chamber with the membrane already placed.

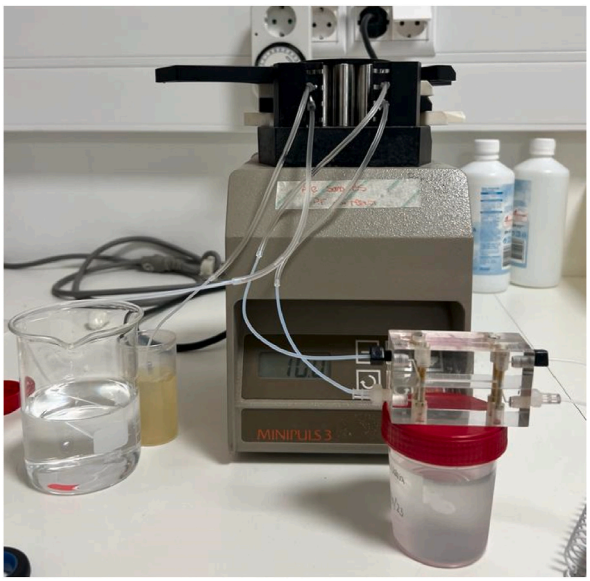

Fig. 5. Schematic of the full process of the HD simulation.

2.6. Degradation tests

Degradation assays were carried out according to studies from Geão et al. and Conde et al. (Geão et al., 2019; Conde et al., 2024). CH-M were trimmed into 2 × 2 cm squares and each piece was weighed. Subsequently, the membranes were submerged in 1 mL of simulated blood fluid containing the same concentrations of urea and albumin as described in section 2.5.1. They remained immersed for 4 h at room temperature. To assess membrane degradation, the membranes were dried in an oven at 60 °C for 24 h and subsequently reweighed.

2.7. In vitro cell studies

2.7.1. Cytotoxicity assay by presto blue

L929 viability assay with presto blue reagent was performed according to ISO 10993-5 (2009). The cells in suspension were seeded at 1×10^4 cells/well in a 96-well plate. Two membranes were tested (CH-M and a PVC one, as control). Metabolic inhibition was assessed using the indirect method, where the membranes remained in contact with the culture medium for 4 h, simulating the standard duration of a HD procedure. Subsequently, aliquots of this medium were added to the cells to determine whether degradation byproducts inhibited cellular metabolism. Finally, fluorescence was measured using a microplate reader after 2 h incubation, and the results were expressed as the percentage of metabolic inhibition relative to the positive control, an inhibition rate exceeding 30 % is

considered cytotoxic.

2.8. Statistical analysis

Statistical analysis was conducted using the IBM® SPSS® Statistics 26 software. For comparing the means across multiple groups, the analysis involved a one-way ANOVA for datasets with a normal distribution, complemented by Tukey's HSD for post hoc analysis. When comparing just two groups, the data underwent analysis with a Student's t-test, if normally distributed. The threshold for statistical significance was established at $p < 0.05$.

3. Results and discussion

3.1. Extraction of chitin and chitosan

The extraction methods for obtaining chitin, and subsequently chitosan, are of critical importance due to their impact on the purity, yield, and functional properties of the final materials. Chitin, a naturally abundant biopolymer found in the exoskeletons of crustaceans, insects, and fungi, requires careful extraction to preserve its structure while removing proteins, minerals, and other impurities. Traditional methods involve demineralization and deproteinization steps, often utilizing acid and alkaline treatments. These processes must be optimized to avoid excessive degradation or alteration of the polymer. The increasing market demand for this biopolymer has driven researchers to look for alternative sources beyond crustaceans, which are subject to seasonal variations and geographic constraints, impacting their availability (Nuc and Dobrzycka-Krahel, 2021). A promising solution emerged with insects, whose exoskeletons are abundantly rich in chitin (Triunfo et al., 2022; Hahn et al., 2022).

The data presented in Table 1 compares the chitin yields from *T. molitor* at two different extraction times and reveals E4 and E8 yields of 5.2 ± 0.8 % and 5.0 ± 0.1 % respectively. The difference in yield is not statistically significant ($p > 0.05$), suggesting that the additional time spent on extraction in E8 does not yield a proportionally higher amount of chitin. A shorter time represents an increase in efficiency, particularly relevant when considering the scale-up of production for commercial purposes, where cost is a crucial factor.

The yield percentages were frequently lower than the reported average range (10–36 %) for crustacean chitin (crab and shrimp) (Machado et al., 2024). For instance, the chitin yield of *Pontascus leptodactylus* and *Faxonius limosus*, two crayfish species, has been reported as 22 ± 2.7 % and 20 ± 3.6 %, respectively (Nuc et al., 2023). But, in contrast, *Saduria entomon*, a Baltic benthic crustacean that was recently investigated for chitin extraction and characterization, exhibited a chitin yield of 14.8 % (Rodriguez-Veiga et al., 2022), which is higher than that of *T. molitor*.

In the other hand, the results presented in this study were consistent with the percentages reported for insect chitin (4.3 % *Brachytrupes portentosus* and 4.92 %–18 % *T. molitor,* depending on the stage of life) (Song et al., 2018). Also, these yield results are in line with previous studies using *Beetle holotrichia* and *Melolontha melolontha*. These reports have indicated a range of values for chitin content from 5.3 % to 16 % (Shin et al., 2019). It is important to keep in mind that the chitin extracted from different insects might vary, depending on the insect species, stage of development, and growth conditions (Abidin et al., 2020).

In order to obtain chitosan from E4 and E8, a deacetylation procedure was used, varying also the deacetylation time (Shin et al., 2019). The first deacetylation lasted 2 h (E4D2, E8D2), giving a total of 6 h and 10 h process, and the second deacetylation took 4 h (E4D4, E8D4), giving an 8 h or 12 h process, respectively.

In essence, the findings from Table 2 reinforce the hypothesis that not only is it possible to derive chitosan from insects like *T. molitor* efficiently, but also that it can be done in a manner that is cognizant of economic and environmental sustainability.

From the data in Table 2, one concludes that extending the deacetylation time from 2 h to 4 h did lead to a significant increase in chitosan yield ($p > 0.05$), indicating that the duration of this procedure is a more critical factor than the duration of the chitin extraction.

The most notable increase in yield was observed when comparing the E4D4 and E8D4 samples to their E4D2 and E8D2 counterparts, highlighting the importance of the deacetylation phase. A longer period for the deacetylation phase allows for a more complete conversion of chitin to chitosan, perhaps due to a more thorough deacetylation process.

Despite the highest yield obtained with the E8D4 sample, further work will clarify whether the longer process is justified.

In conclusion, the findings suggest that optimizing the deacetylation time, rather than the chitin extraction time, may be a more viable strategy for improving yield.

For crustaceans' species, for example, *Pontascus leptodactylus* and *Faxonius limosus* the chitosan yields fall within the range obtained in this study (70 ± 13.0 % and 76 ± 9.0 %) (Nuc et al., 2023). In contrast, *Saduria entomon*, a Baltic benthic crustacean recently investigated for chitosan extraction and characterization, exhibited a chitosan yield of 8.2 % (Rodriguez-Veiga et al., 2022), which is significantly lower than *T. molitor*.

Table 1
Comparison of chitin yield from *T. molitor* at different extraction times.

Sample name	Extraction time (h)	Chitin Yield (%)
E4	4	5.2 ± 0.8 %[a]
E8	8	5.0 ± 0.1 %[a]

The same letters mean no statistically significant differences (p > 0.05).

Table 2
Chitin to chitosan conversion efficiency at different extraction times.

Sample name	Chitin Extraction time (h)	Chitosan Extraction time (h)	Chitosan Yield (%)
E4D2	4	2	66.4 ± 0.2^{a}
E4D4	4	4	73.2 ± 0.1^{b}
E8D2	8	2	65.0 ± 0.8^{a}
E8D4	8	4	79.3 ± 0.8^{c}

[a,b,c] Same letters mean no statistically significant differences ($p > 0.05$).

Nevertheless, in other studies, with differing time conditions, chitosan yields from the insects *Beetle holotrichia* and *Melolontha melolontha* ranged from 4 % to 74 % (Kaya et al., 2014a; Chae et al., 2018), which highlights the value of the extraction processes presented. The yield of chitosan extracted from the cuticles of *T. molitor* larvae was 45.1 % (Machado et al., 2024) which is lower than that reported in this study. However, Machado et al., also reported similar chitosan yields of 75 % (Machado et al., 2024). Additionally, the four chitosan samples obtained showed very similar macroscopic features to commercial chitosan (Fig. 6).

Comparing our results with reported studies, the method presented has a significantly reduced processing time, from 1 ½ days to a timeframe of 6–12 h. Also, by employing a hot alkali treatment for decolorization, the method demonstrates remarkable efficiency in achieving similar macroscopic features to commercial chitosan.

3.2. Molecular characteristics of chitosan

3.2.1. Fourier transform infrared spectroscopy

FTIR spectroscopy plays a crucial role in characterizing chitin and chitosan for membrane design, as it provides valuable insights into their chemical structures and functional groups (Pawlak and Mucha, 2003). FTIR analysis enables the identification of key structural changes during the conversion of chitin to chitosan, particularly through the detection of the degree of acetylation and deacetylation (Liu et al., 2006). By analyzing the characteristic absorption bands, FTIR can confirm the presence of amine, hydroxyl, and acetyl groups, which are essential for determining the biopolymer's solubility, mechanical strength, and biocompatibility (Yasmeen et al., 2016)—critical factors in membrane performance. For membrane design, understanding these molecular features is vital for tailoring the material's properties, such as permeability, surface charge, and interaction with target molecules (Sun et al., 2024). Therefore, FTIR analysis is vital to ensure the precise modification of chitin and chitosan, optimizing their functionality for advanced applications in sustainable HD membranes and other biomedical technologies (Yasmeen et al., 2016).

The FTIR spectra of chitosan and chitin obtained from *T. molitor*, and of commercial chitosan, are compared in Fig. 7. The four samples of chitosan from this work showed FTIR spectra extremely comparable to that of the brand chitosan.

A broad absorption peak centered around 3300 cm^{-1} is observed in the IR spectrum of chitin (E4 and E8), indicating the presence of hydrogen bonding associated with O–H or N–H groups, which are functional groups found in chitin. Additionally, a sharp peak at approximately 1650 cm^{-1} is discerned, signifying the presence of carbonyl (C=O), or potentially conjugated double bond (C=C) groups. Two additional peaks at 1450 cm^{-1} and 1250 cm^{-1} correspond to C–H bending in alkanes and C–O stretching in esters or ethers, respectively, suggesting the existence of these functional groups within the chitin structure. Chitosan E8D4 exhibits absorption peaks in the range of 3000-2850 cm^{-1}, indicative of C–H stretching vibrations in aliphatic (alkane) groups. Furthermore, a distinct peak near 1650 cm^{-1} is observed, implying the presence of carbonyl (C=O) groups or potential double bonds (C=C) within the chitosan molecular framework. Chitosan E8D2 shares similarities with chitin in displaying a broad absorption peak around 3300 cm^{-1}, indicating the presence of O–H or N–H groups and the associated hydrogen bonding. Peaks near 1650 cm^{-1}, akin to chitin, signify the existence of carbonyl (C=O) groups. The appearance of peaks at 1450 cm^{-1} and 1250 cm^{-1} suggests the presence of C–H bending in alkanes and C–O stretching in esters or ethers, corroborating the molecular composition.

Chitosan E4D2 showcases a broad absorption peak around 3300 cm^{-1}, akin to other chitosan samples, suggesting the presence of O–H or N–H groups and associated hydrogen bonding. Chitosan E4D4 manifests sharp peaks within the 3000-2850 cm^{-1} range, signifying C–H stretching vibrations in aliphatic (alkane) groups. The sharpness of these peaks may suggest a more ordered or

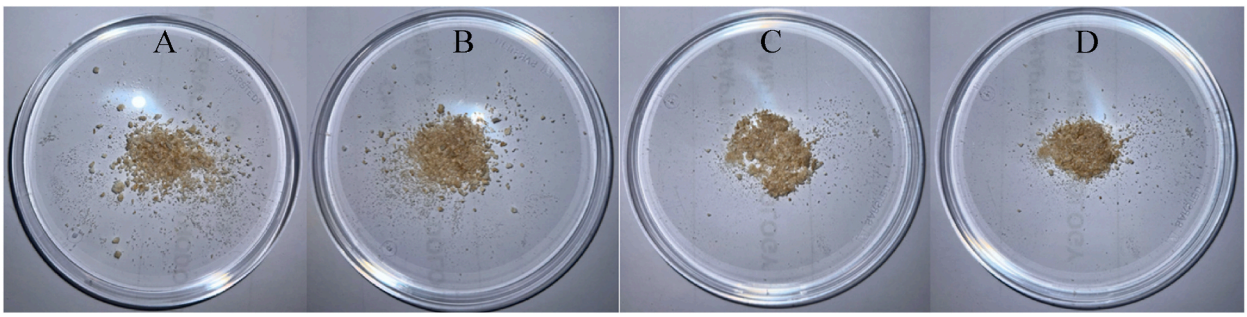

Fig. 6. Macroscopic features of the four chitosan samples. (A) - E4D2; (B) - E4D4; (C) - E8D2; (D) - E8D4.

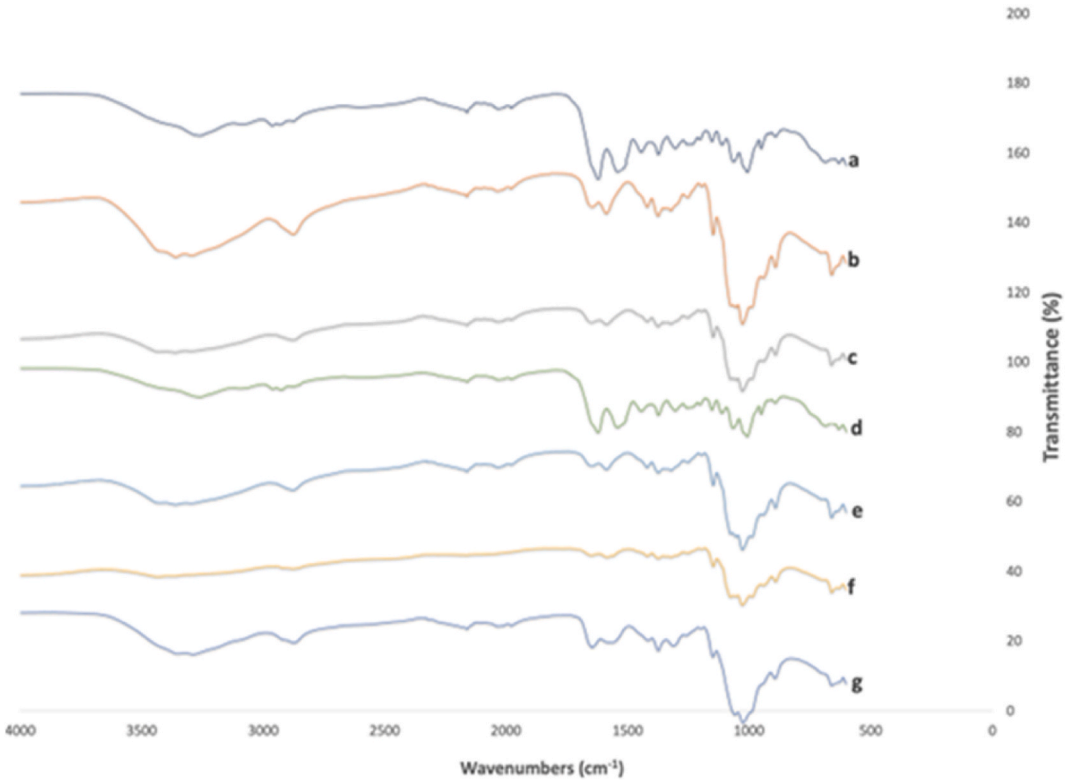

Fig. 7. FTIR spectra of the chitosan and chitin obtained from *T. molitor*: a) chitin (E8); b) chitosan (E8D4); c) chitosan (E8D2); d) chitin (E4); e) chitosan (E4D2); f) chitosan (E4D4); g) commercial chitosan.

crystalline structural arrangement in comparison to other samples, possibly due to differences in processing (Yasmeen et al., 2016; Mahmoud et al., 2014; Varma and Vasudevan, 2020).

3.2.2. *Degree of deacetylation*

Chitosan is produced through deacetylation, a chemical modification where acetyl groups are removed to increase solubility and bioactivity (Aranaz et al., 2021). The effectiveness of the deacetylation process directly influences the DD, which in turn governs the performance of chitosan in various applications, including biomedical and environmental technologies (Ul-Islam et al., 2024). Therefore, refining extraction and deacetylation methods are essential to improve efficiency, sustainability, and the quality of chitin and chitosan for advanced membrane development and other biotechnological uses (Yi et al., 2024).

In general, the amount of alkali solution, reaction temperature, reaction time, and solid chitin structure (Yao et al., 2012) affect the DD. There are two different ways to modify chitin to obtain chitosan: chemically (using intense alkali solutions, alkali catalysis, alkali fusion, and hydrazine hydrate techniques) (Kaya et al., 2014b), and biologically (using enzymes). Since the concentrated alkali solution technique is the most well-known and regularly used due to reduced cost and efficiency, it was selected in this study. To produce chitosan, raw materials were heated in a NaOH solution for 2 h or 4 h. The DD of the four samples of chitosan obtained from *T. molitor* was determined using FTIR and is presented in Table 3.

The E4D2 sample exhibits the highest DD at 75.1 %. Increasing the deacetylation time from 2 h to 4 h had a negligible effect on deacetylation, given that the extraction conditions remained the same.

The E8D2 sample shows a further reduced DD at 73.1 %, indicating that prolonging the chitin extraction time to 8 h may not be optimal for maximizing deacetylation. Also, the E8D4 sample reflects a deacetylation degree of 73.4 %, which is slightly higher than

Table 3
Degree of deacetylation of chitosan samples.

Sample name	Degree of deacetylation (%)
E4D2	75.1
E4D4	74.8
E8D2	73.1
E8D4	73.4
Commercial	70.2

that of E8D2 but still lower than the E4 series.

This could suggest that while extending chitosan extraction time does increase deacetylation, the initial 8 h chitin extraction may limit the potential for higher deacetylation levels.

The commercial sample presents the lowest degree of deacetylation at 70.2 %, which could be due to various factors, including the source of chitin, and industrial processing techniques.

The results obtained are consistent with data previously reported in the literature, which indicates that the DD of medium-molecular-weight commercial chitosan (from crustaceans) ranges from 70 to 85 % and from other insects, such as *Blaps luthier, Pimelia fernandezlopezi, Musca domestica* rages from 86.9 to 88 % (Amor et al., 2023).

3.2.3. Zeta potential

Zeta potential is a key parameter for characterizing chitin and chitosan in membrane design, as it provides critical information about the surface charge and electrostatic behavior of these biopolymers. Measuring the zeta potential helps determine the stability of chitin and chitosan dispersions in solution and their interaction with other charged species. For membrane applications, surface charge influences properties such as adsorption, fouling resistance, and selective permeability. A positive zeta potential, often observed in chitosan due to the presence of protonated amine groups, enhances its interaction with negatively charged molecules or ions, which is vital for applications like ion exchange, and HD. By understanding the zeta potential, it can be optimize the electrostatic properties of chitosan membranes, fine-tuning their functionality for improved performance in filtration, selective transport, and biocompatibility. Hence, zeta potential analysis is essential for designing membranes with enhanced efficiency and tailored surface interactions for advanced HD uses (Athavale et al., 2022).

It stands for the electric surface charge that, as a result of the electrostatic attraction, has a substantial impact on the stability of particles in suspension. A high mutual repulsion between the particles in the medium will prevent particle aggregation when they all have either a noticeably negative or positive zeta potential. Typically, entities with zeta potential greater than +30 mV or lower than −30 mV are regarded as being stable (Warsito and Agustiani, 2021).

The zeta potential of chitosan is a key indicator of its colloidal stability, with higher positive values generally correlating to better electrostatic repulsion, which reduces the risk of aggregation and sedimentation. The high zeta potential value observed in both the commercial (65.5 mV) and produced chitosan samples (average of 58.1 mV) suggests a strong positive surface charge, promoting stability in suspension (Benamer Oudih et al., 2023). This stability is particularly valuable in applications such as drug delivery, wound healing, and tissue engineering, where consistent dispersion and functionality are crucial (Benamer Oudih et al., 2023).

The slight difference between the commercial and produced chitosan zeta potentials could arise from variations in molecular weight, DD, or differences in the processing methods. Produced chitosan with a slightly lower, yet still high, zeta potential (58.1 mV) may offer unique benefits by allowing for customization in applications that demand moderate stability with potential for targeted interactions, such as in responsive drug delivery systems or in formulations where controlled interaction with biological cells is desired (Németh et al., 2022).

3.3. Biological activities of chitosan from Tenebrio molitor

3.3.1. Antimicrobial activity

The antimicrobial activity of chitosan is a critical feature in membrane design, especially for applications in biomedical technologies (Ke et al., 2021). Chitosan's inherent antimicrobial properties arise from its positively charged amine groups, which interact with negatively charged microbial cell membranes, leading to cell disruption and death (Mawazi et al., 2024). This capability is particularly valuable in designing membranes for HD, wound healing, and filtration systems, where preventing bacterial contamination and biofouling is essential (Nguyen et al., 2012). By incorporating chitosan into membrane structures it can be enhance the material's ability to inhibit microbial growth, extending the membrane's lifespan, maintaining its efficiency, and reducing the need for chemical disinfectants. The antimicrobial function also makes chitosan an attractive choice for developing sustainable, biocompatible membranes, minimizing the risks of infection and contamination in clinical and environmental applications (Mawazi et al., 2024). Therefore, the antimicrobial activity of chitosan not only improves the membrane's performance but also contributes to safer and more sustainable filtration and dialysis systems.

The extracted chitosan was evaluated for antimicrobial activity against a wide range of microorganisms associated with infections.

Table 4
MLC values, in mg/mL, of the chitosan samples from *T. molitor* and of commercial chitosan.

	MLC (mg/mL)				
Microorganisms	E8D2	E8D4	E4D2	E4D4	Commercial
MRSA	6	4	4	6	4
MSSA	4	4	2	6	4
Staphylococcus epidermidis	6	2	2	6	4
Escherichia coli	4	4	6	6	4
Pseudomonas aeruginosa	6	6	8	6	6
Candida albicans	2	4	2	4	4

Note: Microbial growth was observed in the tested controls of culture medium and culture medium with acetic acid (1 % v/v).

It was proved that all four chitosan samples are active against *E. coli*, *S. aureus* (MSSA and MRSA), *C. albicans, S. epidermidis*, and *P. aeruginosa*. Table 4 summarizes the MLC values found for each chitosan, including the commercial one.

The MLC is the lowest broth dilution of an antimicrobial compound that prevents the growth on an agar plate. The failure to develop on the plate means that only nonviable microorganisms are available (Abedon et al., 2011).

The antimicrobial agent exhibiting the highest potency is characterized by possessing the lowest MLC value. While all extracted chitosan showed antimicrobial properties similar to the commercial sample, the analysis highlighted E4D2 as having the most significant inhibitory effects, requiring the lowest MLCs against a wide array of microorganisms. It is noted that E4D2 also exhibited a higher DD, aligning with literature that suggests a higher DD correlates with increased antimicrobial activity.

Until now, the antimicrobial activity of insect chitosan has been explored by a limited number of studies, however, there is already some evidence for insects such as *T. molitor* (Shin et al., 2019). The notable antimicrobial properties underscore the potential utilization of chitosan in crafting biodegradable membranes for HD.

3.3.2. Antioxidant activity

The antioxidant activity of chitosan is a significant attribute in membrane design, particularly for biomedical applications where oxidative stress can degrade membrane performance or harm surrounding tissues (Xia et al., 2022). Chitosan's antioxidant properties are primarily due to its ability to scavenge free radicals and inhibit lipid peroxidation, which is vital in preventing oxidative damage (Ivanova and Yaneva, 2020). In HD, membranes are exposed to reactive oxygen species (ROS) that can compromise the functionality of the membrane and contribute to inflammation in patients (Wang et al., 2024). By incorporating chitosan, which neutralizes ROS, membranes can be designed to protect against oxidative stress, enhancing their durability and biocompatibility (Ivanova and Yaneva, 2020). Therefore, the antioxidant activity of chitosan not only improves membrane stability but also offers protective benefits in applications that require long-term use and high oxidative resistance (Herdiana et al., 2023).

Using the ABTS method, the antioxidant activity was assessed, with results shown in Table 5.

The chitosan E8D4, E4D2 and commercial chitosan showed that their antioxidant activities are not significantly different ($p > 0.05$).

The results suggest that the extraction and deacetylation times have no impact on the antioxidant activity of the chitosan.

In conclusion, variations in processing times did not affect the antioxidant properties of chitosan. The antioxidant activity of the commercial chitosan falls within the range of the extracted samples, suggesting that the extraction methodology used for the *T. molitor* samples was not more deleterious.

Also, the observed values are within the range described in the literature, which ranges from 48.5 to 80.9 μmol Trolox equivalent/g for crustacean chitosan (Muñoz-Tebar et al., 2023).

3.4. Membrane development and HD simulation

Simulating HD to monitor key blood biochemical markers, such as urea and albumin, is essential in the design of CH-M for dialysis applications. HD aims to mimic kidney function by efficiently removing waste products, like urea, while retaining essential proteins, such as albumin. In this context, testing the performance of CH-M under simulated HD conditions allows to evaluate their selective permeability, adsorption capacity, and ability to maintain a critical balance between toxin removal and protein retention. Chitosan's natural affinity for specific biomolecules and its tunable surface properties make it a promising material for designing membranes that optimize this filtration process. By simulating real dialysis conditions, it can be assess the membrane's capacity to achieve efficient urea clearance while minimizing albumin loss, thus ensuring that the membrane supports effective toxin removal without compromising patient health. Such simulations are crucial for refining the membrane's structure, improving its clinical performance, and advancing sustainable and biocompatible alternatives for long-term HD treatments (Lee et al., 2022).

It is crucial to note, also, that this setup did not entirely replicate the typical HD process. The membrane used is not of the hollow fiber type, and the experiment did not involve blood contact, nor were hemocompatibility tests conducted. These are important distinctions from the clinical setting and should be taken into consideration when interpreting the results.

As far as our understanding extends, this is the sole flow model (dynamic and counter-current) validated for albumin and urea for simulating HD.

3.4.1. Stability and membrane permeation

For the urea permeation, over a time range of 2–6 min, the analysis demonstrated a consistent permeation of urea across the membrane, with concentrations ranging from 0.27 to 0.31 mg/mL (Table 6), once the initial solution presented a concentration of 0.37 mg/mL.

Table 5
Values of the ABTS antioxidant activity of the produced and commercial chitosan, in μmol TE/g.

	ABTS μmol TE/g			
E8D2	E8D4	E4D2	E4D4	Commercial
62.97 ± 1.35^{b}	65.53 ± 1.42^{a}	65.62 ± 3.22^{a}	60.91 ± 1.45^{b}	64.17 ± 2.61^{a}

[a] [b] Same letters mean no statistically significant differences ($p > 0.05$).

Table 6
Urea permeation through the CH-M.

Time (min)	Urea Permeated (mg/mL)	Urea Permeated (%)
2	0.29 ± 0.02	77.6 ± 5.24
4	0.31 ± 0.01	82.6 ± 3.72
6	0.27 ± 0.00	72.8 ± 0.87

After 2 min, the urea permeated was measured at 0.29 ± 0.019 mg/mL, which equates to 77.6 ± 5.2 %. This high permeation in such a short time underscores the membrane's rapid response to urea diffusion, a critical aspect of HD.

Subsequently, at 4 min, there was a slight increase in both the concentration and percentage of urea permeated, reaching 0.31 ± 0.01 mg/mL and 82.6 ± 3.7 %, respectively. This can suggest that the membrane maintains its permeability over time, allowing for continued diffusion of urea without saturation or loss of function.

After this, at the 6-min interval, there was a slight decrease in urea permeation to 0.27 ± 0.003 mg/mL, which corresponds to 72.8 ± 0.9 % permeation. This reduction could be attributed to the approach towards an equilibrium state, where the concentration gradient between the two sides of the membrane diminishes over time (Suri, 2016).

During a real HD process, approximately 60–70 % of urea is typically removed from the blood. While it is challenging to specify a definitive percentage for adequate dialysis, it is observed that patients tend to have a longer lifespan and fewer hospital admissions when the urea reduction ratio (URR) - a critical measure of the dialysis treatment ability to remove urea from the blood - is 60 % or higher (Suri, 2016).

The choice of these specific time intervals was strategic, aiming to capture the initial efficiency and progression towards equilibrium of the membrane filtration capacity. Nonetheless, the permeability rate is directly proportional to the filtration surface (i.e. filter and/or membrane). In this case, the surface with size 6 × 1 cm allows a test permeability of low volumes and flow rates (i.e. 1.5 mL/min), and consequently a few minutes (i.e. less than 10 min), until establishing its equilibrium. Therefore, this was a pilot permeability test that is still far from real dialysis conditions.

In this study, when analyzing the samples collected at 2, 4, and 6-min intervals, it was observed a complete absence of albumin in the filtrate. This was conclusively verified through BCA assay, which displayed no deviation from the baseline, clearly indicating the CH-M effectiveness in retaining albumin molecules.

The ability of the membrane to selectively filter solutes while preventing the passage of larger molecules like albumin is of paramount importance in its application in HD.

In typical HD processes, not all albumin is retained and, according to the literature, dialysis-related albumin loss is up to 26.4 g/4 h.

The ability of a dialyzer to sieve or reject solutes during dialysis has been known as a marker for the clinician to determine the suitable dialyzer for the patient. The sieving coefficient (that indicates the potential of different solutes to pass across a particular dialyzer membrane) is < 0.001 for albumin for the most common commercial PSu dialyzers (Said et al., 2019).

The study revealed total albumin retention by the CH-M, suggesting a very high level of selectivity. Also, a degradation of 12.5 % was observed within the HD conventional simulated time of 4 h. Although this does not indicate cytotoxicity levels (as shown in Section 3.5), it underscores the need for further optimization studies to enhance chitosan crosslinking within the membrane, ensuring improved structural integrity and performance. Within this and despite these promising results, several limitations must be recognized. Firstly, the time frame of the analysis was relatively short, restricted to intervals of 2, 4, and 6 min. This duration may not fully capture the membrane performance over the extended periods typical of HD treatments, as mentioned previously. Secondly, while the focus on albumin retention was critical, it does not cover the entire spectrum of molecules that are involved in HD, thereby necessitating a more comprehensive range of testing for a thorough evaluation. Furthermore, the study was conducted under laboratory conditions, which may not completely reflect the complexities encountered in a clinical HD setup.

Another significant limitation was the absence of actual blood contact in the performance tests, a factor that is essential in real-world HD scenarios and can significantly impact the performance of the membrane. Lastly, the study did not include hemocompatibility tests, which are crucial for assessing how the membrane interacts with blood components in clinical applications (Ji et al., 2023).

Understanding these limitations is vital for interpreting the results within the appropriate context and for guiding future research aimed at optimizing the membrane design and functionality for practical HD applications.

Nonetheless, this study provides us with a conceptual examination validating the semi-permeable capacity of the membrane for molecules with both higher and lower molecular weights.

3.5. Citotoxicity

Cytotoxicity testing was conducted on L929 cells to assess the impact of the samples on cell metabolism, utilizing a viability dye. Fig. 8 assesses the metabolic inhibition induced by two types of membrane samples: CH-M and a PVC-based control. The metric of metabolic inhibition serves as an indicator of cytotoxicity, CH-M sample exhibited 20.36 ± 8.11 % metabolic inhibition. This suggests some impact on cell metabolism, yet it remains well below the cytotoxic threshold. On the other hand, the PVC sample did not demonstrate metabolic inhibition, effectively close to zero, with minimal variability, underlining its high biocompatibility.

According to ISO 10993-5 (2009) standards, a sample is considered cytotoxic if it causes metabolic inhibition greater than 30 % (International Organization of Standardization, 2009). Given that, neither the CH-M nor PVC membranes exceed this threshold, they

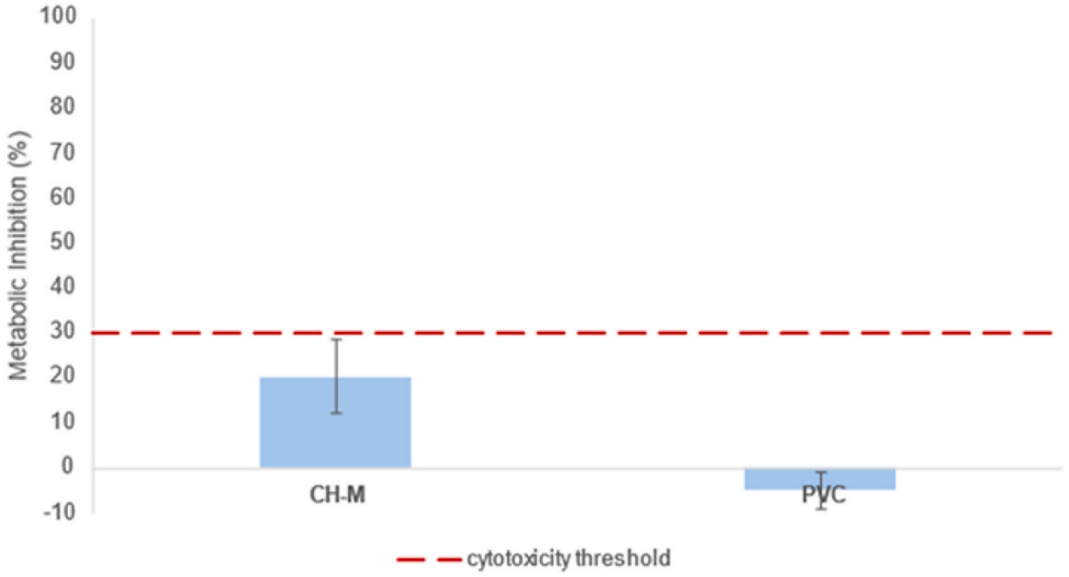

Fig. 8. Analysis of cytotoxic effects in CH-M and PVC membranes on L929 fibroblast cells.

are not classified as cytotoxic.

Nevertheless, the presence of chitosan in the CH-M membrane correlates with increased metabolic inhibition compared to the PVC membrane. In fact, chitosan is known for its bioactive properties, which can interact with cellular components leading to higher metabolic inhibition (Croisier and Jérôme, 2013). Also, this interaction can be due to chitosan's inherent biological activities which include antimicrobial effects and its ability to induce minimal inflammatory responses, affects cell metabolism (Dai et al., 2011).

The CH-M sample, despite showing some level of metabolic inhibition, does not reach a level that would raise concerns over its biocompatibility, potentially allowing for its use in applications where minimal interaction with cells is crucial, such as in components of HD membranes. This initial data supports the potential of these materials in medical applications, warranting further investigation to fully assess their suitability for specific medical uses as HD (Bhattarai et al., 2010).

4. Conclusions

This work serves as a foundation for future investigations and advancements in the field, encouraging the continuation of research efforts to innovate in sustainable medical HD technologies.

Hereupon, chitin extraction from *T. molitor* and conversion to chitosan were carried out with significantly reduced processing times. The analyses of the extraction times for obtaining both chitin and chitosan show that a longer time does not necessarily result in a higher yield. This finding is particularly relevant for the industrial scalability of chitosan production, where time efficiency directly correlates with economic viability.

The physicochemical characterization of chitosan, along with the bioactive assessments through antimicrobial and antioxidant activities, has provided a diverse overview of the material properties. Chitosan derived from *T. molitor* demonstrated noteworthy activity against a variety of microorganisms, including bacteria Gram-positive, bacteria Gram-negative, and yeast. This antimicrobial activity alongside its antioxidant capacity evaluated through ABTS radical scavenging, shows chitosan potential in biomedical applications, particularly in the realm of sustainable HD membranes. These membranes, given their antimicrobial ability, open the range of possible reusable membranes in the HD area, which promises to be sustainably disruptive.

Despite some permeation tests being conducted, the study did not fully explore expanding permeability tests for other components beyond urea and albumin. Extending these tests over longer periods could also provide a more comprehensive understanding of the membrane's performance under varied conditions. This research on insect-derived chitosan, particularly from *T. molitor*, represents a highly sustainable and renewable resource that is not commercially available, contrasting with traditional sources such as crustaceans, which face environmental and supply chain limitations. Furthermore, it holds the potential to recast the existing paradigm of HD membranes.

CRediT authorship contribution statement

Maria Martingo: Writing – original draft, Methodology, Formal analysis, Conceptualization. **Sara Baptista-Silva:** Writing – review & editing, Visualization, Validation, Supervision, Methodology, Investigation, Conceptualization. **Raquel Mesquita:** Writing – review & editing, Visualization, Validation, Methodology. **João Paulo Ferreira:** Writing – review & editing, Visualization, Validation. **Sandra Borges:** Writing – review & editing, Visualization, Validation, Supervision, Methodology, Investigation, Conceptualization.

Manuela Pintado: Writing – review & editing, Validation, Project administration, Funding acquisition, Conceptualization.

Declaration of competing interest

The authors declare that they have no known competing financial interests or personal relationships that could have appeared to influence the work reported in this paper.

Acknowledgements

This work was supported by National Funds from project BUGS@PETS (POCI-01-0247-FEDER-047042) funded by Fundo Europeu de Desenvolvimento Regional (FEDER), under Programa Operacional Competitividade e Internacionalização (POCI). We would also like to thank the scientific collaboration from Fundação para a Ciência e a Tecnologia (FCT) through project UIDB/50016/2020.

Data availability

The authors do not have permission to share data.

References

Abedon, S., 2011. In: Laskin, A.I., Sariaslani, S., Gadd, G.M.B.T.-A. (Eds.), Chapter 1 - Phage Therapy Pharmacology: Calculating Phage Dosing, 77. Academic Press, pp. 1–40.
Aberoumand, A., Chabavi, M., 2024. Extraction and quality control of chitin and chitosan from shrimp (Vanami) litophenause vanamei shells wastes. Nat. Prod. Commun. 19.
Aberoumand, A., Muolenejad, F., 2024. Production and quality control of chitin and chitosan from shrimp (Farfantepenaeus notialis) shells obtained from Hendijan, Iran by sequence process. Journal of Research in Agriculture and Food Sciences 1, 108.
Abidin, N.A.Z., Kormin, F., Abidin, N.A.Z., Anuar, N.A.F.M., Bakar, M.F.A., 2020. The potential of insects as alternative sources of chitin: an overview on the chemical method of extraction from various sources. Int. J. Mol. Sci. 21, 1–25. https://doi.org/10.3390/ijms21144978. Preprint at.
Amor, I. Ben, Hemmami, H., Laouini, S.E., Abdelaziz, A.G., Barhoum, A., 2023. Influence of chitosan source and degree of deacetylation on antibacterial activity and adsorption of AZO dye from water. Biomass Convers Biorefin. https://doi.org/10.1007/s13399-023-03741-9.
Aranaz, I., et al., 2021. Chitosan: an overview of its properties and applications. Polymers 13. https://doi.org/10.3390/polym13193256. Preprint at.
Athavale, R., et al., 2022. Tuning the surface charge properties of chitosan nanoparticles. Mater. Lett. 308, 131114.
Benamer Oudih, S., et al., 2023. Chitosan nanoparticles with controlled size and zeta potential. Polym. Eng. Sci. 63, 1011–1021.
Bhattarai, N., Gunn, J., Zhang, M., 2010. Chitosan-based hydrogels for controlled, localized drug delivery. Adv. Drug Deliv. Rev. 62, 83–99. https://doi.org/10.1016/j.addr.2009.07.019. Preprint at.
Biagini, G., et al., 1994. Fibroblast proliferation over dialysis membrane: an experimental model for “tissue” biocompatibility evaluation. Int. J. Artif. Organs 17, 620–628.
Bonomini, M., Piscitani, L., Di Liberato, L., Sirolli, V., 2022. Biocompatibility of surface-modified membranes for chronic hemodialysis therapy. Biomedicines 10. https://doi.org/10.3390/biomedicines10040844. Preprint at.
Bowry, S.K., Chazot, C., 2021. The scientific principles and technological determinants of haemodialysis membranes. Clinical Kidney Journal 14, I5–I16. https://doi.org/10.1093/ckj/sfab184. Preprint at.
Chae, K.S., Shin, C.S., Shin, W.S., 2018. Characteristics of cricket (Gryllus bimaculatus) chitosan and chitosan-based nanoparticles. Food Sci. Biotechnol. 27, 631–639.
Conde, A., et al., 2024. A crayfish chitosan-based bioactive film to treat vaginal infections: a sustainable approach. Int. J. Biol. Macromol. 277.
Coscueta, E.R., Reis, C.A., Pintado, M., 2020. Phenylethyl isothiocyanate extracted from watercress by-products with aqueous micellar systems: development and optimisation. Antioxidants 9. https://doi.org/10.3390/antiox9080698. Preprint at.
Coscueta, E.R., Sousa, A.S., Reis, C.A., Pintado, M., 2021. Chitosan-olive oil microparticles for phenylethyl isothiocyanate delivery: optimal formulation. PLoS One 16.
Croisier, F., Jérôme, C., 2013. Chitosan-based biomaterials for tissue engineering. Eur. Polym. J. 49, 780–792. https://doi.org/10.1016/j.eurpolymj.2012.12.009. Preprint at.
Czechowska-Biskup, R., et al., 2012. Progress on Chemistry and Application of Chitin and its, XVII.
Dai, T., Tanaka, M., Huang, Y.Y., Hamblin, M.R., 2011. Chitosan preparations for wounds and burns: antimicrobial and wound-healing effects. Expert Review of Anti-Infective Therapy 9, 857–879. https://doi.org/10.1586/eri.11.59. Preprint at.
Edo, G.I., Yousif, E., Al-Mashhadani, M.H., 2024. Chitosan: an overview of biological activities, derivatives, properties, and current advancements in biomedical applications. Carbohydr. Res. 542.
EFSA Panel on Nutrition, N. F. and F. A. (NDA), 2021. Safety of dried yellow mealworm (Tenebrio molitor larva) as a novel food pursuant to Regulation (EU) 2015/2283. EFSA J. 19, e06343.
Foreman, K.J., et al., 2018. Forecasting life expectancy, years of life lost, and all-cause and cause-specific mortality for 250 causes of death: reference and alternative scenarios for 2016&2013. Lancet 392, 2052–2090.
Fox, A. & Franklin, G. Clinical Practice Guideline Haemodialysis. www.nice.org.uk/accreditation.
Fresenius Medical Care. Facts & Figures, 2023.
Geão, C., et al., 2019. Thermal annealed silk fibroin membranes for periodontal guided tissue regeneration. J. Mater. Sci. Mater. Med. 30.
Hahn, T., et al., 2022. Purification of chitin from pupal exuviae of the black soldier fly. Waste Biomass Valorization 13, 1993–2008.
Herdiana, Y., Husni, P., Nurhasanah, S., Shamsuddin, S., Wathoni, N., 2023. Chitosan-based nano systems for natural antioxidants in breast cancer therapy. Polymers 15. https://doi.org/10.3390/polym15132953. Preprint at.
Hestekin, C.N., et al., 2023. High flux novel polymeric membrane for renal applications. Sci. Rep. 13, 11703.
International Organization of Standardization, 2009. ISO 10993–5 (2009) - Biological Evaluation of Medical Devices.
Ivanova, D.G., Yaneva, Z.L., 2020. Antioxidant properties and redox-modulating activity of chitosan and its derivatives: biomaterials with application in cancer therapy. Biores Open Access 9, 64–72.
Ji, H., et al., 2023. Advances in enhancing hemocompatibility of hemodialysis hollow-fiber membranes. Advanced Fiber Materials 5, 1198–1240. https://doi.org/10.1007/s42765-023-00277-5. Preprint at.
Kaya, M., et al., 2014a. Comparison of physicochemical properties of chitins isolated from an insect (Melolontha melolontha) and a crustacean species (Oniscus asellus). Zoomorphology 133, 285–293.
Kaya, M., Seyyar, O., Baran, T., Turkes, T., 2014b. Bat guano as new and attractive chitin and chitosan source. Front. Zool. 11, 59.
Ke, C.L., Deng, F.S., Chuang, C.Y., Lin, C.H., 2021. Antimicrobial actions and applications of Chitosan. Polymers 13. https://doi.org/10.3390/polym13060904. Preprint at.

Kumar Gupta, G., De, S., Franco, A., Balu, A.M., Luque, R., 2015. Sustainable biomaterials: current trends, challenges and applications. Molecules 21, E48. https://doi.org/10.3390/molecules21010048. Preprint at.
Kumirska, J., Weinhold, M.X., Thöming, J., Stepnowski, P., 2011. Biomedical activity of chitin/chitosan based materials—influence of physicochemical properties apart from molecular weight and degree of N-acetylation. Polymers 3, 1875–1901. https://doi.org/10.3390/polym3041875. Preprint at.
Lee, S., Sirich, T.L., Meyer, T.W., 2022. Improving solute clearances by hemodialysis. Blood Purif. 51, 20–31. https://doi.org/10.1159/000524512. Preprint at.
Liu, D., Wei, Y., Yao, P., Jiang, L., 2006. Determination of the degree of acetylation of chitosan by UV spectrophotometry using dual standards. Carbohydr. Res. 341, 782–785.
Machado, S.S.N., et al., 2024. Insect residues as an alternative and promising source for the extraction of chitin and chitosan. Int. J. Biol. Macromol. 254.
Mahmoud, A.A., et al., 2014. FTIR spectroscopy of natural bio - polymers blends. Journal o f Applied Sciences 4, 816–824.
Mawazi, S.M., Kumar, M., Ahmad, N., Ge, Y., Mahmood, S., 2024. Recent applications of chitosan and its derivatives in antibacterial, anticancer, wound healing, and tissue engineering fields. Polymers 16. https://doi.org/10.3390/polym16101351. Preprint at.
Mei, Z., Kuzhir, P., Godeau, G., 2024. Update on chitin and chitosan from insects: sources, production, characterization, and biomedical applications. Biomimetics 9. https://doi.org/10.3390/biomimetics9050297. Preprint at.
Mesquita, R.B.R., Rangel, A.O.S.S., 2005. Gas Diffusion Sequential Injection System for the Spectrophotometric Determination of Free Chlorine with O-Dianisidine. In Talanta, 68. Elsevier, pp. 268–273.
Muñoz-Tebar, N., Pérez-Álvarez, J.A., Fernández-López, J., Viuda-Martos, M., 2023. Chitosan edible films and coatings with added bioactive compounds: antibacterial and antioxidant properties and their application to food products: a review. Polymers 15. https://doi.org/10.3390/polym15020396. Preprint at.
Németh, Z., et al., 2022. Quality by design-driven zeta potential optimisation study of liposomes with charge imparting membrane additives. Pharmaceutics 14.
Nguyen, T., Roddick, F.A., Fan, L., 2012. Biofouling of water treatment membranes: a review of the underlying causes, monitoring techniques and control measures. Membranes 2, 804–840. https://doi.org/10.3390/membranes2040804. Preprint at.
Nuc, Z., Dobrzycka-Krahel, A., 2021. From chitin to chitosan – a potential natural antimicrobial agent. Progress on Chemistry and Application of Chitin and its Derivatives 26, 23–40. https://doi.org/10.15259/PCACD.26.003. Preprint at.
Nuc, Z., et al., 2023. Pontastacus leptodactylus (Eschscholtz, 1823) and Faxonius limosus (Rafinesque, 1817) as new, alternative sources of chitin and chitosan. Water (Switzerland) 15.
Pawlak, A., Mucha, M., 2003. Thermogravimetric and FTIR studies of chitosan blends. Thermochim. Acta 396, 153–166.
Ravi Kumar, M.N.V., 2000. A review of chitin and chitosan applications. React. Funct. Polym. 46, 1–27.
Rodriguez-Veiga, I., Acosta, N., Aranaz, I., Dobrzycka-Krahel, A., 2022. Exploring Saduria entomon (Crustacea Isopoda) as a new source for chitin and chitosan isolation. Int. J. Mol. Sci. 23.
Rose, I.I., et al., 2022. Single-step chitosan functionalized membranes for heparinization. J Memb Sci 655.
Safavi, A., Thrastardottir, R., Thorarinsdottir, R.I., Unnthorsson, R., 2024. Insect production: a circular economy strategy in Iceland. Sustainability 16.
Said, N., et al., 2019. Iron oxide nanoparticles improved biocompatibility and removal of middle molecule uremic toxin of polysulfone hollow fiber membranes. J. Appl. Polym. Sci. 136.
Shin, C.-S., Kim, D.-Y., Shin, W.-S., 2019. Characterization of chitosan extracted from Mealworm Beetle (Tenebrio molitor, Zophobas morio) and Rhinoceros Beetle (Allomyrina dichotoma) and their antibacterial activities. Int. J. Biol. Macromol. 125, 72–77.
Song, Y.S., et al., 2018. Extraction of chitin and chitosan from larval exuvium and whole body of edible mealworm, Tenebrio molitor. Entomol. Res. 48, 227–233.
Sun, S., Li, S., Wang, S., Chen, Y., 2024. Design and development of highly selective and permeable membranes for H2/CO2 separation—a review. Chem. Eng. J. 494. https://doi.org/10.1016/j.cej.2024.152972. Preprint at.
Suri, R.S., 2016. KDOQI Hemodialysis Adequacy Clinical Practice Guideline Update 2015: what You Need to Know Presentation for National Renal Administrators' Association.
Szymańska, E., Winnicka, K., 2015. Stability of chitosan - a challenge for pharmaceutical and biomedical applications. Mar. Drugs 13, 1819–1846. https://doi.org/10.3390/md13041819. Preprint at.
Triunfo, M., et al., 2022. Characterization of chitin and chitosan derived from Hermetia illucens, a further step in a circular economy process. Sci. Rep. 12.
Ul-Islam, M., et al., 2024. Chitosan-based nanostructured biomaterials: synthesis, properties, and biomedical applications. Advanced Industrial and Engineering Polymer Research 7, 79–99. https://doi.org/10.1016/j.aiepr.2023.07.002. Preprint at.
Varma, R., Vasudevan, S., 2020. Extraction, characterization, and antimicrobial activity of chitosan from Horse Mussel Modiolus modiolus. ACS Omega 5, 20224–20230.
Wang, Z., et al., 2024. Effect of chitosan and its water-soluble derivatives on antioxidant activity. Polymers 16.
Warsito, M.F., Agustiani, F., 2021. A review on factors affecting chitosan nanoparticles formation. In: IOP Conference Series: Materials Science and Engineering, 1011. IOP Publishing Ltd.
Xia, Y., et al., 2022. Applications of chitosan and its derivatives in skin and soft tissue diseases. Front. Bioeng. Biotechnol. 10. https://doi.org/10.3389/fbioe.2022.894667. Preprint at.
Yao, K., Li, J., Yao, F., Yin, Y., 2012. Chitosan-Based Hydrogels. Taylor & Francis Group, LLC.
Yasmeen, S., Kabiraz, M., Saha, B., Qadir, M., Gafur, M., 2016. Chromium (VI) ions removal from Tannery Effluent using chitosan-microcrystalline cellulose composite as adsorbent. Int. Res. J. Pure Appl. Chem. 10, 1–14.
Yi, K., Miao, S., Yang, B., Li, S., Lu, Y., 2024. Harnessing the potential of chitosan and its derivatives for enhanced functionalities in food applications. Foods 13. https://doi.org/10.3390/foods13030439. Preprint at.
Zainol Abidin, N.A., Kormin, F., Zainol Abidin, N.A., Mohamed Anuar, N.A.F., Abu Bakar, M.F., 2020. The potential of insects as alternative sources of chitin: an overview on the chemical method of extraction from various sources. Int. J. Mol. Sci. 21.